




## Article

# Cosmeceutical Potentials of *Grammatophyllum speciosum* Extracts: Anti-Inflammations and Anti-Collagenase Activities with Phytochemical Profile Analysis Using an Untargeted Metabolomics Approach

Yodying Yingchutrakul <sup>1,2</sup>, Wattanapong Sittisaree <sup>3</sup>, Thanisorn Mahatnirunkul <sup>4</sup>, Thitikorn Chomtong <sup>4</sup>,  
Tatpong Tulyananda <sup>5</sup> and Sucheewin Krobthong <sup>2,6,7,\*</sup>

<sup>1</sup> National Omics Center, NSTDA, Pathum Thani 12120, Thailand; yodying.yin@nstda.or.th

<sup>2</sup> Center for Neuroscience, Faculty of Science, Mahidol University, Bangkok 10400, Thailand

<sup>3</sup> Merck Life Science Thailand, Merck Ltd., Bangkok 10110, Thailand;

wattanapong.sittisaree@external.merckgroup.com

<sup>4</sup> National Nanotechnology Center, NSTDA, Pathum Thani 12120, Thailand;

thanisorn.mah@nanotec.or.th (T.M.); thitikorn.cho@nanotec.or.th (T.C.)

<sup>5</sup> School of Bioinnovation and Bio-Based Product Intelligence, Faculty of Science, Mahidol University, Bangkok 10400, Thailand; tatpong.tul@mahidol.edu

<sup>6</sup> Department of Biochemistry, Faculty of Science, Mahidol University, Bangkok 10400, Thailand

<sup>7</sup> Interdisciplinary Graduate Program in Genetic Engineering, Kasetsart University, Bangkok 10900, Thailand

\* Correspondence: sucheewin.k@ku.th or sucheewin82@gmail.com; Tel.: +66-(8)-044-23282



**Citation:** Yingchutrakul, Y.; Sittisaree, W.; Mahatnirunkul, T.; Chomtong, T.; Tulyananda, T.; Krobthong, S. Cosmeceutical

Potentials of *Grammatophyllum speciosum* Extracts:

Anti-Inflammations and

Anti-Collagenase Activities with Phytochemical Profile Analysis Using an Untargeted Metabolomics

Approach. *Cosmetics* **2021**, *8*, 116.

<https://doi.org/10.3390/cosmetics8040116>

Academic Editors: Da-Wei Huang, Antonio Vassallo, Po Hsien Li and Wen-Lung Kuo

Received: 3 November 2021

Accepted: 7 December 2021

Published: 9 December 2021

**Publisher's Note:** MDPI stays neutral with regard to jurisdictional claims in published maps and institutional affiliations.



**Copyright:** © 2021 by the authors. Licensee MDPI, Basel, Switzerland. This article is an open access article distributed under the terms and conditions of the Creative Commons Attribution (CC BY) license (<https://creativecommons.org/licenses/by/4.0/>).

**Abstract:** *Grammatophyllum speciosum* is the largest orchid species and a well-known traditional medicinal plant. Due to skin aging, natural products that inhibit this process can attract the attention of consumers and scientists because radical-scavenging activity, collagenase inhibition, and inflammatory suppression are valuable in dermatological applications. This study investigated the phytochemicals in *G. speciosum* leaves extracts that have cosmeceutical potentials, including radical-scavenging, anticollagenase, and anti-inflammatory abilities. *G. speciosum* leaves were extracted using water-based extraction methods. High-resolution mass spectrometry was used to identify the phytochemicals in the extracts. Fibroblast and keratinocyte cell cytotoxicity was determined. Antioxidant abilities were measured using DPPH and ABTS assays. The effect of the extracts on nitric oxide (NO) in macrophage cells was investigated. ELISA of the collagenase enzyme was determined. A total of 721 annotated metabolites were identified in the extracts. Vitexin and orientin were the most abundant metabolites. Cell viability was >80% in both cell lines when the extract concentration was <1 mg/mL. The IC<sub>50</sub> values for DPPH and ABTS were 56 and 117 µg/mL, respectively. Furthermore, the extracts revealed that NO and collagenase activity were suppressed by 42% and 23%, respectively. The extracts can suppress ROS, inflammatory, and collagenase activities without causing fibroblast and keratinocyte cell death. Thus, this study provides information on metabolites in *G. speciosum* leaves, which is promising as cosmeceuticals or pharmaceuticals with anti-inflammatory and anti-collagenase activities.

**Keywords:** anti-inflammatory; antioxidants; nitric oxide; cosmeceuticals; fibroblast; HaCat; LC-MS/MS

## 1. Introduction

Skin aging occurs because collagen decreases in connective tissue, resulting in a loss of strength and flexibility in the skin. An alteration of the connective tissue structures and functions manifests as skin shriveling and wrinkles. Many stresses, both intrinsic and extrinsic inducers can accelerate the aging process of the skin. The predominant extrinsic inducers of reactive oxygen species (ROS) generation are ultraviolet exposure, pollution, and specific matter. Furthermore, ROS has a direct effect on melanocyte cells in the inner

skin layer by enhancing skin pigmentation through the melanogenesis pathway. High levels of ROS promote fluctuation in the expression level of several protein types in the connective tissue, which contributes to skin aging [1]. Furthermore, ROS primarily targets macromolecules, such as proteins, lipids, and genetic materials, such as DNA and RNA, resulting in cellular stresses and being associated with multiple skin diseases, cancers, and inflammation-related diseases [2].

Prolonged high ROS levels are also associated with inflammatory processes. ROS, especially nitric oxide (NO), can activate prostaglandin-endoperoxide synthase in skin erythema, which are crucial enzymes for prostaglandin E2 synthesis, and thereby stimulate the inflammatory response [3]. NO was generated by the NO synthase enzyme and inhibited NO synthase decreased NO levels, which reduced skin erythema [4]. Under prolonged ROS situations, inflammation cascade was activated via numerous signaling proteins, for example, iNOS, PTGS2, cytokines, and IL-6, IL-1 $\beta$ , and TNF- $\alpha$ , which are produced by immune cells. Additionally, the MAPK-signaling pathway and AP-1 transcription factor of inflammatory proteins can stimulate other inflammatory proteins, accelerating the inflammation response and even resulting in skin damage or aging [5–7]. Therefore, discovering novel radical-scavenging compounds would be beneficial for human health. The inhibition of oxidative stress or inflammatory mediators can be a solution to slow down the skin aging process.

Several antioxidant compounds, such as gallic acid, ascorbic acid, or peptides enhanced cell resistance to ROS and prevent skin inflammation [8,9]. Although there are synthetic antioxidant compounds, such as butylated hydroxyanisole, tertiary butylhydroquinone, and butylated hydroxytoluene, the adverse effects of these compounds limit their use in cosmeceutical products [10,11]. Some of the research now focuses on identifying harmless natural antioxidants safe for humans and produced using green processes.

Bioactive compounds in cosmeceutical applications can be extracted from natural materials using various approaches. Alcohol extraction is a general solvent used for extracting plant materials. However, the extraction processes require less environmentally friendly organic solvents. Water extraction (WE) is one of the most promising green extraction techniques. A single extraction that reduces the number of steps in a process results in lower investment costs and time. A short extraction period also prevents some bioactive components from degrading. Another advantage of WE is the applicability for both large-scale (industrial) and small-scale (laboratory) systems. In addition, using WE techniques in various medical plants also revealed antioxidant and anti-inflammatory activities [12]. The bioactive compound from the ethanolic extract in *G. speciosum* exhibited radical-scavenging ability and wound healing in fibroblasts [13]. The methanolic extract of *G. speciosum* contains several secondary metabolites, such as vitexin, isovitexin, gastodin,  $\gamma$ -tophyllsides, cronupapine, orcinol glucoside, vanilloloside [14]. Most of these compounds revealed multi-functional properties beneficial for skin cells. *G. speciosum* extract may be useful for cosmeceutical ingredients or pharmaceutical applications due to its benefits. *G. speciosum* is a plant of the Orchidaceae family that is predominantly found in Thailand. *G. speciosum* extract is used in various cosmeceutical applications, such as reducing radical-induced cell death in human keratinocyte (HaCaT) cells and stimulating wound healing in fibroblasts [13]. Due to its benefits, these phytochemicals in this plant may be used as cosmetic ingredients. However, the phytochemical profile of WE with antioxidative stress, anti-inflammatory, and anti-collagenase activities has not been investigated.

Metabolome-based LC-MS/MS analysis was a valuable tool for discovering phytochemicals in plants. Characterization of metabolites from the traditional plants has inspired the development of cosmeceutical products. The overall procedure in the discovery of natural compounds with bio-functionalities typically starts with extractions and screening of crude extracts, followed by the identification of the major and active compounds [15]. The use of LC-MS/MS in metabolite profiling demonstrated numerous benefits, including high sensitivity, small sample volume, and compatibility with other chromatographic

techniques, such as size-exclusion chromatography, ion-exchange [16]. Another significant advantage of LC-MS/MS-based metabolomics was the fragment ion search (FISh) function in Compound Discoverer™ software, which provides useful information for structural elucidation and comparison with known metabolite databases. These approaches provide a good method for mining useful chemical information in natural products, resulting in an important tool for quality evaluation in terms of robustness, confidentiality, and efficacy. In this study, we present the first information on water-based phytochemical profiles in *G. speciosum* leaves with antioxidative stress, anti-inflammatory, and anti-collagenase activity, which is promising as a functional cosmetic ingredient for developing phytomedicinal products.

## 2. Materials and Methods

### 2.1. Reagents, Chemicals, Materials, and Solvents

*G. speciosum* fresh leaves were collected in May 2021 in Pathumthani, Thailand with a specific geological indication (14.01764, 100.53213). Materials and equipment used in this study were purchased from several places, including a vacuum blender (BL181D31) from TEFAL Co. (Bangkok, Thailand), a rotatory evaporation R-300 from Buchi Co. (Flawil 1, Switzerland). A FilterMax F5 microplate reader was purchased from BioTek Co. (Winooski, VT, USA), Vivaspin® 20 was purchased from GE Healthcare Co. (Amersham, UK), Benchtop centrifuge (Sorvall™ Legend™ Micro 17), FilterMax F5 microplate reader, and Hypersil GOLD™ C18 column (2.1 × 10 mm, 1.9 μm) were purchased from Thermo Scientific Co. (Waltham, MA, USA). Sep-Pak C18 cartridges (SPE) and Waters extraction manifold system were obtained from Waters Co. (Milford, MA, USA).

The American Type Culture Collection (Manassas, VA, USA) supplied fibroblast cells (ATCC TIB-71), keratinocyte cells (HaCat), and RAW264.7 cells (TIB-71). Biochemical reagents, including Dulbecco's Modified Eagle Medium (DMEM) and Fetal Bovine Serum (FBS) were purchased from Gibco (Grand Island, NY, USA). The penicillin G, dimethyl sulfoxide (DMSO), MTT, LPS, IFNγ, and Griess reagent were obtained from Sigma Aldrich Co. (St. Louis, MO, USA). Collagenase Inhibitor Screening Kit (ab211108) was purchased from Abcam., All other reagents were purchased from Sigma Aldrich Co. Solvents for LC-MS, including water and acetonitrile (LC-MS grade) were purchased from J.T. Baker (Fisher Scientific, Loughborough, UK).

### 2.2. Phytochemicals Extracts Preparation and Quality Control

*G. speciosum* fresh leaves (10 g) were mixed with 90 mL of deionized water (DI) ground using the vacuum blender for 45 s. The suspension was incubated for 3 h at 37 °C with a shaker at 150 rpm. Then, the solution was centrifuged at 14,000 × g for 30 min at 8 °C. SPE with the extraction manifold system was used to clean up the clear upper solution. SPE was pre-conditioned using 20 mL of acetonitrile and equilibrated with 50 mL of water. The supernatants were loaded on the equilibrated SPE and eluted by 99% acetonitrile/water. The elutes were then evaporated under a vacuum using rotatory evaporation. To confirm the phytochemical content, the experiments were conducted in two-biological replications. The samples were reconstituted in 200 μL methanol and diluted with 1800 μL of 1% formic acid/water at 1:10 ratio (*v/v*) before being subjected to LC-MS/MS analysis. Quality control of *G. speciosum* extract was conducted for confirming the reproducibility data, we used the LC-MS/MS approach to determine the total ion intensity of all identified compounds from two independent extraction batches (*n* = 2).

### 2.3. Phytochemical Profiles Analysis Using LC-MS/MS

Phytochemical analysis using a Thermo Q-Exactive Quadrupole Orbitrap Mass Spectrometer, coupled with an UltiMate 3000 LC system. Hypersil GOLD™ column held at 40 °C was used to separate the analytes. A total of 5 μL sample injections (1 μg/ μL) were used at a flow rate of 0.3 mL/min. The column and auto-sampler temperatures were maintained at 40 °C and 8 °C, respectively. The mobile phase was composed of 95%/5%

methanol/water with 0.1% formic acid (MP:A), and acetonitrile with 0.1% formic acid (MP:B) (LC-MS grade, Sigma). Gradient starting conditions were 99% MP: A and 1% MP: B. Starting conditions were held for 2 min before rising to 55% B over 25 min. The column was flushed with 99% B for 5 min before returning to the starting conditions. The total time of each analysis was 35 min. A blank sample (0.1% formic acid/water) was administered after every injection. MS was operated in a positive mode. A spray voltage of 3.8 kV in both positive, sheath gas, and auxiliary gas flow rates were set at 48 and 11 arbitrary units (AU), respectively. The capillary temperature was 350 °C. The MS analysis alternated between MS full scans and data-dependent MS/MS scans with dynamic exclusion. LC-MS for full MS: scan range, 90–800  $m/z$ ; resolution 240,000; AGC target  $3 \times 10^6$ ; max IT 100 ms and LC-MS for full MS/MS, resolution 30,000; AGC target  $1 \times 10^5$ ; max IT 200 ms. Up to six ions (Top6) with the most intense signal were fragmented. All LC-MS runs were acquired using the Xcalibur 3.1 software (Thermo Scientific, Waltham, MA, USA). The TIC profiles of all raw files were analyzed using MZmine 2 software [17].

#### 2.4. Data Processing for Phytochemicals Identification

The acquired raw MS files were processed with the Compound Discoverer 3.1 (Thermo Fisher Scientific, Waltham, MA, USA) to identify phytochemicals. Peak identification, peak alignment, and peak feature extraction were all conducted in a positive mode on the data. The retention time (RT) and mass-to-charge ratio ( $m/z$ ) of different injections were conducted according to the retention time deviation of 0.5 min and the mass deviation of 5 ppm. Then, the peak extraction was performed according to the set information and adduct information: mass deviation =5 ppm, signal strength deviation = 30%, signal-to-noise ratio =2, and fine isotopic pattern matching >90% of the precursor and the characteristic product ions. Additionally, the peak area was quantified. The target  $m/z$  ions were then integrated to predict the molecular formula, which was compared to mzCloud (<https://www.mzcloud.org>; accessed on 1 November 2021) and ChemSpider (<http://www.chemspider.com>; accessed on 1 November 2021) online databases for the identification and confirmation of the compounds. Furthermore, structural elucidation and transformations were suggested for each chromatographic peak by the FISH function. The FISH coverage score was calculated, and fragments on the MS/MS spectrum were auto-annotated with structure, molecular weight, and elemental composition. Among candidate metabolites obtained from mzCloud and ChemSpider with FISH, the highest MS/MS coverage scores were selected for annotation. The candidate metabolites with annotation and had mzCloud best match score >50 and FISH coverage >20 or area > $1 \times 10^9$  AU were reported.

#### 2.5. Extracts' Effects on Fibroblast and Keratinocyte Cells

Cell cytotoxicity of the extracts was evaluated using an MTT assay. The dried extracts were freshly dissolved in a culture medium before the experiments. The human fibroblasts and keratinocyte cells were cultured in DMEM containing 10% FBS and 100 IU/mL of penicillin in a humidified environment containing 5% CO<sub>2</sub> at 37 °C. Briefly, the cells were seeded at a density of  $2 \times 10^4$  cells per well in a 96-well plate. The cells were examined for cytotoxicity at various concentrations (8, 4, 2, 1, 0.5, 0.25, 0.125, 0.063 mg/mL) of the extracts and culture medium as control for 24 h. Next, we measured the optical absorbance at 570 nm using the microplate reader and transformed the results into the cell survival rate percentage. The experiments were conducted in triplicate ( $n = 3$ ).

#### 2.6. In Vitro Antioxidant Assays Using DPPH and ABTS Assays

For DPPH scavenging activity, 10  $\mu$ L of the extracts were mixed with 190  $\mu$ L DPPH solution (0.2 mM in methanol). The control sample contains 20  $\mu$ L of methanol and 200  $\mu$ L of DPPH (0.2 mM). For ABTS scavenging activity, ABTS radical solution (7-mM ABTS stock solution with 2.45 mM potassium persulfate) was diluted in 5 mM phosphate buffer saline pH 7.4, to acquire an absorbance of approximately 0.50 at 734 nm before performing the assay. The extract (10  $\mu$ L) was mixed with 190  $\mu$ L of ABTS solution. The reaction was

incubated at room temperature in the dark for 10 min. The absorbance of the mixture was evaluated at 734 nm. The extract's percentage scavenging capacity was expressed in IC<sub>50</sub> values, which denote the extract concentration required to scavenge 50% of DPPH and ABTS free radicals. Both experiments were conducted in triplicate ( $n = 3$ ).

### 2.7. Collagenase Inhibition Assay Using Enzyme-Linked Immunosorbent Assay

The collagenase inhibitor screening kit was used to measure the enzyme activity to determine the extracts' effect on collagenase activity. The testing sample was solubilized with DI and diluted with kit assay buffer (CAB). The collagenase enzyme was freshly dissolved in CAB before the experiments. The test samples were prepared by mixing the tested extract with collagenase. The control reactions were prepared using collagenase and buffer only. The activity of the enzyme was determined by a  $\lambda_{\text{excitation}}$  at 490 nm and  $\lambda_{\text{emission}}$  of 520 nm using the microplate reader. The measurement was made at an endpoint, for 60 min at 37 °C. All samples were prepared in two biological replicates and three experimental triplicates. The ability to inhibit collagenase activity by the analyzed samples was calculated from the equation:

$$\% \text{enzyme activity} = \frac{(\text{Em}\lambda_{\text{control}} - \text{Em}\lambda_{\text{sample}})}{\text{Em}\lambda_{\text{control}}} \times 100\% \quad (1)$$

where  $\text{Em}\lambda_{\text{sample}}$  denotes the reaction absorbance with the testing sample and  $\text{Em}\lambda_{\text{control}}$  denotes the reaction absorbance without the testing sample. The experiment was conducted in triplicate ( $n = 3$ ).

### 2.8. NO Determination Level Using Griess Assay

NO level was used to evaluate the potential of the extracts on anti-inflammatory effect. RAW264.7 cells were plated in a 96-well plate ( $5 \times 10^4$  cells/well) overnight, followed by the addition of 10 U/mL, IFN- $\gamma$ , and 100 ng/mL LPS for 24 h in the presence or absence (control) of the extract (100 and 20  $\mu\text{g/mL}$ ). To analyze NO production, 120  $\mu\text{L}$  of supernatant was incubated with an equal volume of Griess solution at room temperature for 10 min before reading absorbance at 540 nm. Since NO content was reflected by the amount of nitrite, a calibration curve was generated using sodium nitrite. The calibration curve was used to calculate the amount of nitrite in the supernatants. Percentage NO suppression by the extract was expressed in IC<sub>50</sub> values, which denote the extract concentration required to reduce 50% NO level. All experiments were conducted in triplicate ( $n = 3$ ).

### 2.9. Statistical Analysis

All experiments were conducted with at least three independent replicates ( $n = 3$ ), the results were reported as mean  $\pm$  standard deviation (SD) and analyzed with GraphPad Prism software. One-way analysis of variance (one-way ANOVA) was performed using PD for proteomics software. Duncan's multiple range test ( $p < 0.05$ ) was used to determine the significance of differences.

## 3. Results and Discussions

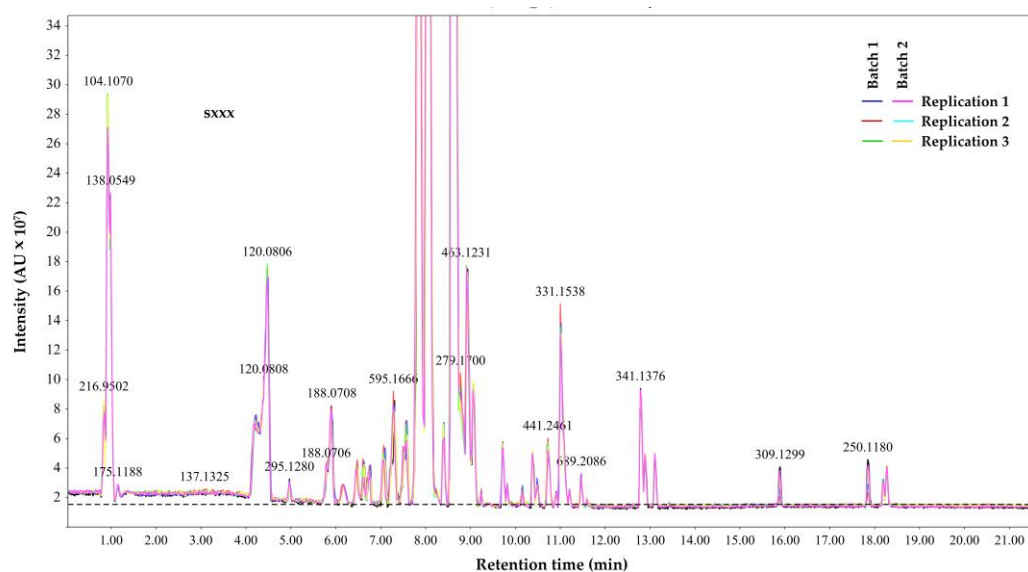
### 3.1. Phytochemical Profiling and Metabolite Qualitative Analysis

The extraction solvents used in dermatological products should take into account primarily human health requirements; the water extraction used is safe for human health. Our extraction method does not have to demonstrate organic solvent absence throughout the extraction process, and water is not a safety concern.

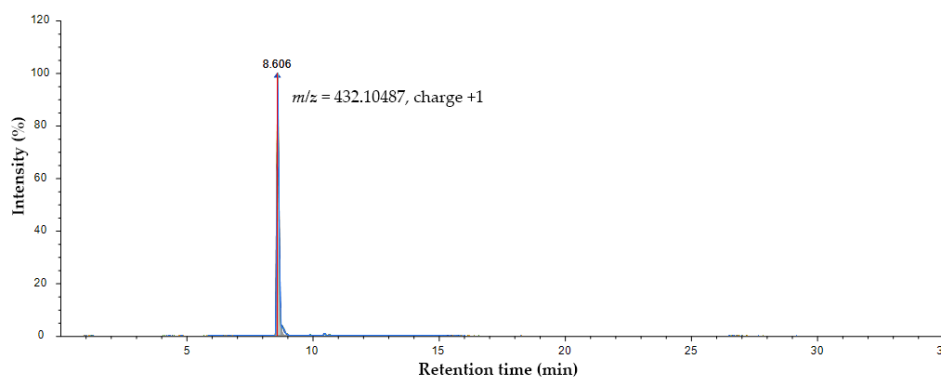
The accuracy of phytochemical profiles data highly depends on the biological sampling and LC-MS/MS instrument performance. To examine whether the instrument is in good operating condition and whether the sample preparation and method applied were appropriate, the TIC of all injections is shown in Figure 1A. Furthermore, the highest peaks



of each injection (two bio-replication and three experimental replication) are extracted from the TIC, as shown in Figure 1B.



(A)



(B)

**Figure 1.** LC-MS/MS phytochemical profiles of *G. speciosum* extracts. (A) Aligned TIC profiles of the extracts in six LC runs of 35 min. The TIC building was achieved using a minimum height of  $1 \times 10^5$  and maximum height at  $3.5 \times 10^8$ , (B) Aligned extracted ion chromatogram (XIC) of the highest peak ( $m/z = 432.10487$ , charge +1) detected in the positive mode in six LC runs with full-range retention time (RT). Unit of X-axis and Y-axis are minutes and percentage intensity abundance, respectively.

TIC of independent batches and technical replicates revealed consistency and reproducibility. The XIC reproducibility of  $m/z = 432.10487$  at approximately 8.6 was shown in six LC-MS runs. Additionally, this peak exhibited good symmetry and was consistent across the two batches of the experiments (compound coefficient of variance per sample batch as 2%). Additionally, the TIC of all the detected metabolites in the six LC runs revealed that their profiles are extremely comparable in terms of elution time and intensity values, indicating consistency and reproducibility in batches at the overall level.

The identification of metabolites by LC-MS/MS with HCD in a positive mode is well-established. A total of 721 annotated phytochemical species were identified using WE for *G. speciosum*. Table 1 lists the top ten phytochemicals associated with the KEGG pathway.

**Table 1.** List of high abundance phytochemicals detected in *G. speciosum* extracts.

Phytochemicals	Formular	Mass (Da)	Area (AU)	CV. (%) <sup>a</sup>	KEGG Pathway
Vitexin	C <sub>21</sub> H <sub>20</sub> O <sub>10</sub>	432.105	1.88 × 10 <sup>10</sup>	1.79	Flavone and flavonol biosynthesis
Orientin	C <sub>21</sub> H <sub>20</sub> O <sub>11</sub>	448.100	7.32 × 10 <sup>9</sup>	1.52	Flavone and flavonol biosynthesis
3-[(1E)-1-propen-1-yl]pyridine	C <sub>8</sub> H <sub>9</sub> N	119.073	2.68 × 10 <sup>9</sup>	17.11	-
Phenylacetylene	C <sub>8</sub> H <sub>6</sub>	102.047	1.86 × 10 <sup>9</sup>	10.76	-
5,7-dihydroxy-2-(3-hydroxy-4-methoxyphenyl)-4-oxo-4H-chromen-3-yl-6-deoxy-α-L-mannopyranoside	C <sub>22</sub> H <sub>22</sub> O <sub>11</sub>	462.116	1.82 × 10 <sup>9</sup>	15.63	-
Choline	C <sub>5</sub> H <sub>13</sub> NO	103.100	1.37 × 10 <sup>9</sup>	2.87	-
Arginine	C <sub>6</sub> H <sub>14</sub> N <sub>4</sub> O <sub>2</sub>	174.112	1.23 × 10 <sup>9</sup>	2.02	Biosynthesis of plant secondary metabolites
Histidinediium	C <sub>6</sub> H <sub>11</sub> N <sub>3</sub> O <sub>2</sub>	157.085	1.22 × 10 <sup>9</sup>	2.01	-
Phenylacetylene	C <sub>8</sub> H <sub>6</sub>	102.047	1.15 × 10 <sup>9</sup>	22.74	-
Trigonelline	C <sub>7</sub> H <sub>7</sub> NO <sub>2</sub>	137.048	1.11 × 10 <sup>9</sup>	2.3	Biosynthesis of phenylpropanoids Biosynthesis of alkaloids derived from shikimate pathway

<sup>a</sup> coefficients of variation values in all biological replicate groups ( $n = 2$ ) and technical replicate groups ( $n = 3$ ) for each metabolite.

We discovered that vitexin and orientin were major components associated with plant flavone and flavonol biosynthesis pathways (ID: map00941). It could imply that flavone and flavonol compounds constituted most phytochemicals in WE. The additional MS2 spectrum obtained from HCD combined with the FiSH algorithm enabled us to obtain the annotated phytochemical compounds information. The presence of these annotated compounds was confirmed and validated using their respective accurate mass, experimental and calculated  $m/z$ , molecular formula, precursor mass error, MS2 fragmentation pattern, and well-known database matching.

Different extraction solvents affected phytochemical profiling of *G. speciosum*. The other extraction solvent, such as ethanol, provides gastrodin as a major component [13]. Gastrodin is a phenolic glycoside that has antiosteoporosis properties and a reduction in cellular ROS [18]. However, our results do not show gastrodin, so we can deduce that different extraction solvents produce different phytochemical profiles. The biological compounds derived from *G. speciosum* extracts are important in discovering novel therapeutic bioactive compounds and the synthesis of new potential cosmeceuticals. Biological components of the extracts, such as glycosides, tannins, flavonoids, alkaloids, saponins, and coumarins from the plants can have a synergistic effect and produce desirable pharmacological effects for health [19]. Based on this evidence, it may be implied that the antioxidative stress mechanism of *G. speciosum* WE took a different path due to vitexin and orientin being major components. Different phytochemical species provide an opportunity to discover new bio-related activities.

### 3.2. Effects of Extracts on Fibroblasts and HaCat Cells

The evaluation of cell cytotoxicity is a crucial issue in producing extracts for practical use in cosmeceutical applications. The cytotoxicity of the extracts was studied in the fibroblasts and keratinocyte cell lines as normal skin cells. MTT assay was used to evaluate cell cytotoxicity following a 48 h treatment with extracts, as shown in Figure 2.

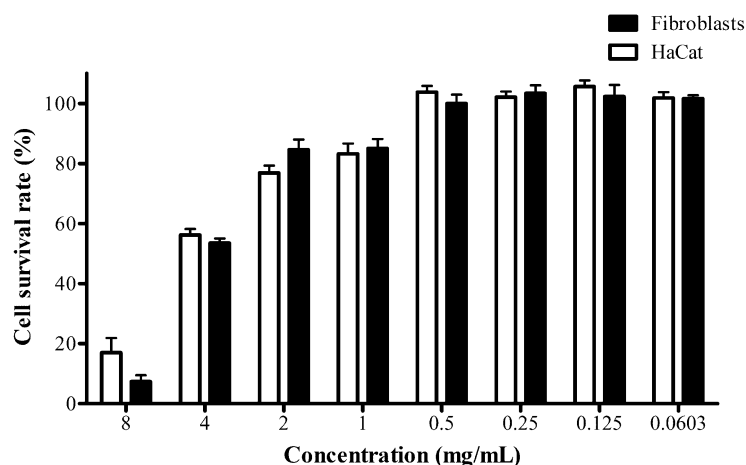


**Figure 2.** Concentration-dependent effect of the extract on fibroblasts and HaCat cell viability using MTT assay. Fibroblasts as (■) and HaCat cells as (□) were incubated with 8–0.06 mg/mL extract for 24 h. Data were shown as mean  $\pm$  SD from triplicate results.

Although the model in this study is mouse melanoma cells, cell cytotoxicity analysis indicated several cell deaths in a concentration-dependent manner, therefore, supporting the hypothesis that inflammatory and collagenase activity can be suppressed and radical-scavenging activity can increase without affecting cell viability.

*G. speciosum* WE concentration in the range of 0.0603–0.5 mg/mL exhibited insignificant cell death in all testing cell lines compared to the untreated control. The ethanolic extraction of *G. speciosum* was studied for its cytotoxicity to the fibroblast cells. A concentration range of 5–100  $\mu$ g/mL showed no toxicity to the fibroblast cells (cell survival rate >90%) [13]. Our results revealed that at 500  $\mu$ g/mL of the extracts did not affect fibroblast and HaCat cells when using WE for extraction. Because the extracts' toxicity to skin cells would be lower in cosmeceutical products, the concentration with no observed cell death was evaluated in collagenase and inflammatory studies. Therefore, the concentration we used in both studies is 100  $\mu$ g/mL, which did not affect fibroblast and HaCat cell viability.

### 3.3. Antioxidant Capacity Measurement of Extracts Using DPPH and ABTS Assays

Since the antioxidant capacity of the extracts should be estimated using multiple assays to determine radical-scavenging ability [20], the in vitro radical-scavenging potential of the extracts was determined using two methods: DPPH and ABTS assays. These assays were used because they are widely employed in screening antioxidant abilities and primarily characterize antioxidative compounds [9,21]. The extracts at various concentrations of 10, 20, 40, 80, 160  $\mu$ g/mL, were used to conduct these assays. The IC<sub>50</sub> of scavenging activities of DPPH and ABTS were 56 and 117  $\mu$ g/mL ( $R^2$  for DPPH and ABTS were 0.999 and 0.991, respectively). Its effect was comparable with ascorbic acid and gallic acid which are well-known antioxidants widely used in cosmetic products [8].

We used both antioxidant assays because the extracts contained various types of phytochemicals. Furthermore, the radical-scavenging capacities were differences stemming from solubility issues of radicals and their spreading rate in each solvent. Overall, DPPH can be completely dissolved in alcoholic solvents and is capable of accepting electrons, as well as hydrogens, whereas ABTS can be completely solubilized in water and other organic media [22]. Hence, the antioxidant capacity of DPPH and ABTS in the extracts can be measured for both hydrophilic and hydrophobic compounds.

The results supported *G. speciosum* as a potentially promising cosmetic natural ingredient commonly used as anti-aging serum [23]. The present study provided useful information about the antioxidant capacity of the extracts, which might be beneficial as a cosmetic ingredient for the prevention of ROS formation.



### 3.4. Collagenase Activity Determination by ELISA Assay

Collagenase plays important roles in the degradation of collagen proteins. Therefore, it is important to find promising agents that could inhibit the degradation of collagens. A fluorometric assay was used to measure the extracts that modulate collagenase activity in the presence of extracts (100 µg/mL) was measured. The extracts had a distinct inhibitory effect compared to the control. The collagenase-inhibitory effect of the extracts was  $25.41\% \pm 2.18\%$  compared to the control ( $p$ -value  $\leq 0.01$ ). The inhibitory effects of the extracts may be primarily attributed to their rich source of vitexin and orientin.

This extract affects inhibition of the collagenase enzyme. This enzyme hydrolyzed collagen proteins within the skin, hence, collagenase-inhibitory activity can reduce collagen degradation. As we know collagen is a major constituent of dermal connective tissue, many scientists have characterized inhibitors of this enzyme, which will prevent the loss of structural integrity and flexibility in the skin. Antioxidant compounds can prevent collagen degradation caused by free radicals [24]. These findings can imply that the extracts were collagenase inhibitors and might be beneficial in reducing collagen degradation via scavenging radical abilities.

### 3.5. Effects of Extracts on NO Level in Macrophage Cells

Due to NO being a regulator of inflammatory processes, we determined the effect of the extracts on NO level in RAW264.7 cells. The  $IC_{50}$  value of the extracts was 98 µg/mL ( $R^2 = 0.997$ ) compared to PBS (control condition) used in the experiment. To determine whether the extracts modulated the NO, the cells were treated with extracts (100 µg/mL), and the culture medium was collected to evaluate NO levels. The extracts had a distinct inhibitory effect compared to the control. The NO level of the extracts was 50.49% compared to the control ( $p$ -value  $\leq 0.01$ ), as shown in Figure 3.

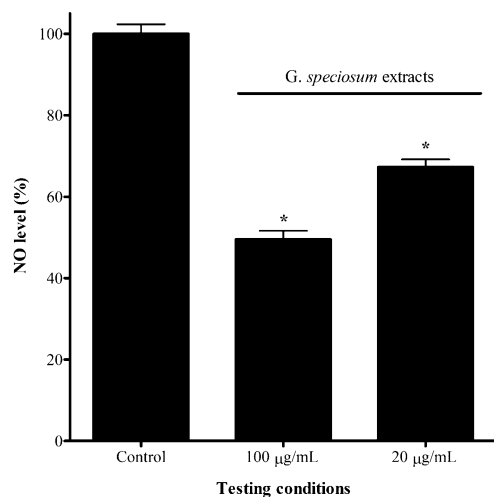


**Figure 3.** NO release by LPS-induced RAW267 cells and treated with the extract. The cells were treated with extract at concentrations of 100 and 20 µg/mL. Data are represented as mean  $\pm$  SD from triplicate results. The number of asterisks (\*) denotes the significance levels ( $p < 0.01$ ) compared to the control condition.

In healthcare products, potential adverse effects of nitric oxide inhibition should be considered. Nitric oxide inhibition could be harmful to patients with cardiovascular and renal diseases. Nitric oxide is cardio-protective during ischemic events by causing coronary vasodilation and enhancing oxygen delivery. Additionally, nitric oxide inhibition suppresses statin-induced oxygen delivery to the myocardium.

NO is crucial in mediating several aspects of inflammatory responses in nearly every organ system including the skin. Increased NO level at skin cells is demonstrated in atopic dermatitis, irritant dermatitis, allergic dermatitis, skin swelling, and sunburn-induced

flushing [25]. Furthermore, NO nitric oxide could be a major factor for causing the redness and inflammation of vascular rosacea [26]. However, a high level of NO inhibition may have side effects and this issue should be a concern. NO inhibition revealed adverse effects in patients with cardiovascular disease, as it can suppress oxygen delivery in the system [27]. To strike a balance between the beneficial and adverse effects, we reduced the concentration of the extract to 20 µg/mL and measured the NO level. The results revealed NO level was reduced 32.72% compared to control ( $p$ -value  $\leq 0.01$ ). These results indicated that we could adjust the concentration of the extracts with the highest beneficial and lowest undesirable effects for developing in demagogical products.

#### 4. Conclusions

The phytochemical profiles of water-based *G. speciosum* extract were determined. LC-MS/MS, 721 annotated metabolites, among them vitexin and orientin are major components. The extract exhibited radical scavenging, NO suppression, and an inhibitory effect on collagenase without affecting the viability of skin cells. Our study shed light on the function of *G. speciosum* extract. This information is valuable for developing natural anti-aging functions for application in cosmetic ingredients.

**Author Contributions:** Conceptualization, S.K.; Data curation, W.S., T.M. and T.T.; Funding acquisition, S.K.; Investigation, T.M., T.C. and T.T.; Methodology, W.S., T.M., T.C. and T.T.; Project administration, S.K.; Resources, T.M.; Software, Y.Y.; Supervision, Y.Y.; Validation, T.C.; Visualization, Y.Y.; Writing—original draft, Y.Y. and S.K.; Writing—review & editing, Y.Y. and S.K. All authors have read and agreed to the published version of the manuscript.

**Funding:** This research received no external funding.

**Institutional Review Board Statement:** Not applicable.

**Informed Consent Statement:** Not applicable.

**Data Availability Statement:** Not applicable.

**Acknowledgments:** We are grateful to Arthit Chairoungduafor (Physiology, Mahidol University, Thailand) and Patompon Wongtrakoongate (Biochemistry, Mahidol University, Thailand) for helpful suggestions and discussions.

**Conflicts of Interest:** The authors declare no conflict of interest.

#### References

1. Brennan, M.; Bhatti, H.; Nerusu, K.C.; Bhagavathula, N.; Kang, S.; Fisher, G.J.; Varani, J.; Voorhees, J.J. Matrix metalloproteinase-1 is the major collagenolytic enzyme responsible for collagen damage in UV-irradiated human skin. *Photochem. Photobiol.* **2003**, *78*, 43–48. [[CrossRef](#)]
2. Gogineni, V.; Hamann, M.T. Marine natural product peptides with therapeutic potential: Chemistry, biosynthesis, and pharmacology. *Biochim. Biophys. Acta Gen. Subj.* **2018**, *1862*, 81–196. [[CrossRef](#)] [[PubMed](#)]
3. Rhodes, L.E.; Belgi, G.; Fau-Parslew, R.; Parslew, R.; Fau-McLoughlin, L.; McLoughlin, L.; Fau-Clough, G.F.; Clough Gf Fau-Friedmann, P.S.; Friedmann, P.S. Ultraviolet-B-induced erythema is mediated by nitric oxide and prostaglandin E2 in combination. *J. Investig. Dermatol.* **2001**, *117*, 880–885. [[CrossRef](#)] [[PubMed](#)]
4. Warren, J.B. Nitric oxide and human skin blood flow responses to acetylcholine and ultraviolet light. *FASEB J.* **1994**, *8*, 247–251. [[CrossRef](#)]
5. Chauhan, P.; Shakya, M. Modeling signaling pathways leading to wrinkle formation: Identification of the skin aging target. *Indian J. Derm. Venereol. Leprol.* **2009**, *75*, 463–468. [[CrossRef](#)]
6. Subedi, L.; Lee, T.H.; Wahedi, H.M.; Baek, S.H.; Kim, S.Y. Resveratrol-enriched rice attenuates UVB-ROS-induced skin aging via downregulation of inflammatory cascades. *Oxid. Med. Cell. Longev.* **2017**, *2017*, 8379539. [[CrossRef](#)]
7. Kim, A.L.; Labasi, J.M.; Zhu, Y.; Tang, X.; McClure, K.; Gabel, C.A.; Athar, M.; Bickers, D.R. Role of p38 MAPK in UVB-induced inflammatory responses in the skin of SKH-1 hairless mice. *J. Invest. Derm.* **2005**, *124*, 1318–1325. [[CrossRef](#)]
8. Masaki, H. Role of antioxidants in the skin: Anti-aging effects. *J. Derm. Sci.* **2010**, *58*, 85–90. [[CrossRef](#)]
9. Krobthong, S.; Yingchutrakul, Y. Identification and enhancement of antioxidant P1-peptide isolated from *Ganoderma lucidum* hydrolysate. *Food Biotechnol.* **2020**, *34*, 338–351. [[CrossRef](#)]
10. Pop, A.; Kiss, B.; Loghin, F. Endocrine disrupting effects of butylated hydroxyanisole (BHA—E320). *Clujul Med.* **2013**, *86*, 16–20.

11. Camarasa, J.G.; Serra-Baldrich, E. Exogenous ochronosis with allergic contact dermatitis from hydroquinone. *Contact Dermat.* **1994**, *31*, 57–58. [[CrossRef](#)] [[PubMed](#)]
12. Wu, L.C.; Jou, A.F.; Chen, S.H.; Tien, C.Y.; Cheng, C.F.; Fan, N.C.; Ho, J.A. Antioxidant, anti-inflammatory and anti-browning activities of hot water extracts of oriental herbal teas. *Food Funct.* **2010**, *1*, 200–208. [[CrossRef](#)]
13. Harikarnpakdee, S.; Chowjarean, V. *Grammatophyllum speciosum* ethanolic extract promotes wound healing in human primary fibroblast Cells. *Int. J. Cell Biol.* **2018**, *2018*, 7836869. [[CrossRef](#)]
14. Sahakitpichan, P.; Mahidol, C.; Disadee, W.; Chimnoi, N.; Ruchirawat, S.; Kanchanapoom, T. Glucopyranosyloxybenzyl derivatives of (R)-2-benzylmalic acid and (R)-eucomic acid, and an aromatic glucoside from the pseudobulbs of *Grammatophyllum speciosum*. *Tetrahedron* **2013**, *69*, 1031–1037. [[CrossRef](#)]
15. Wolf, D.; Siems, K. Burning the hay to find the needle—Data mining strategies in natural product dereplication. *CHIMIA Int. J. Chem.* **2007**, *61*, 339–345. [[CrossRef](#)]
16. Alonso, A.; Marsal, S.; Julia, A. Analytical methods in untargeted metabolomics: State of the art in 2015. *Front. Bioeng. Biotechnol.* **2015**, *3*, 23. [[CrossRef](#)]
17. Du, X.; Smirnov, A.; Pluskal, T.; Jia, W.; Sumner, S. Metabolomics data preprocessing using ADAP and MZmine 2. *Methods Mol. Biol.* **2020**, *2104*, 25–48. [[CrossRef](#)]
18. Huang, Q.; Shi, J.; Gao, B.; Zhang, H.-Y.; Fan, J.; Li, X.-J.; Fan, J.-Z.; Han, Y.-H.; Zhang, J.-K.; Yang, L.; et al. Gastrodin: An ancient Chinese herbal medicine as a source for anti-osteoporosis agents via reducing reactive oxygen species. *Bone* **2015**, *73*, 132–144. [[CrossRef](#)]
19. Milugo, T.K.; Omosa, L.K.; Ochanda, J.O.; Owuor, B.O.; Wamunyokoli, F.A.; Oyugi, J.O.; Ochieng, J.W. Antagonistic effect of alkaloids and saponins on bioactivity in the quinine tree (*Rauvolfia caffra* sond.): Further evidence to support biotechnology in traditional medicinal plants. *BMC Complement. Altern. Med.* **2013**, *13*, 285. [[CrossRef](#)]
20. Mau, J.L.; Chao, G.R.; Wu, K.T. Antioxidant properties of methanolic extracts from several ear mushrooms. *J. Agric. Food Chem.* **2001**, *49*, 5461–5467. [[CrossRef](#)]
21. Krobthong, S.; Choowongkamon, K.; Suphakun, P.; Kuaprasert, B.; Samutrtai, P.; Yingchutrakul, Y. The anti-oxidative effect of Lingzhi protein hydrolysates on lipopolysaccharide-stimulated A549 cells. *Food Biosci.* **2021**, *41*, 101093. [[CrossRef](#)]
22. Shalaby, E.A.; Shanab, S.M.M. Comparison of DPPH and ABTS assays for determining antioxidant potential of water and methanol extracts of *Spirulina platensis*. *Indian J. Geo-Mar. Sci.* **2013**, *42*, 556–564.
23. Chowjarean, V.; Phiboonchaiyanan, P.P.; Harikarnpakdee, S.; Tengamnuay, P. A natural skin anti-ageing serum containing pseudobulb ethanolic extract of *Grammatophyllum speciosum*: A randomized double-blind, placebo-controlled trial. *Int. J. Cosmet. Sci.* **2019**, *41*, 548–557. [[CrossRef](#)] [[PubMed](#)]
24. Madan, K.; Nanda, S. In-vitro evaluation of antioxidant, anti-elastase, anti-collagenase, anti-hyaluronidase activities of safranal and determination of its sun protection factor in skin photoaging. *Bioorg. Chem.* **2018**, *77*, 159–167. [[CrossRef](#)]
25. Bruch-Gerharz, D.; Ruzicka, T.; Kolb-Bachofen, V. Nitric oxide in human skin: Current status and future prospects. *J. Invest. Derm.* **1998**, *110*, 1–7. [[CrossRef](#)] [[PubMed](#)]
26. Qureshi, A.A.; Lerner, L.H.; Lerner, E.A. From bedside to the bench and back. Nitric oxide and the cutis. *Arch. Derm.* **1996**, *132*, 889–893. [[CrossRef](#)] [[PubMed](#)]
27. Janatuinen, T.; Laakso, J.; Laaksonen, R.; Vesalainen, R.; Nuutila, P.; Lehtimäki, T.; Raitakari, O.T.; Knuuti, J. Plasma asymmetric dimethylarginine modifies the effect of pravastatin on myocardial blood flow in young adults. *Vasc. Med.* **2003**, *8*, 185–189. [[CrossRef](#)] [[PubMed](#)]